Biochemical and Biophysical Research Communications 425 (2012) 781–787

Contents lists available at SciVerse ScienceDirect

Biochemical and Biophysical Research Communications

journal homepage: www.elsevier.com/locate/ybbrc

CARMA3 is overexpressed in colon cancer and regulates NF-κB activity and cyclin D1 expression

Zhifeng Miao, Tingting Zhao, Zhenning Wang, Yingying Xu, Yongxi Song, Jianhua Wu, Huimian Xu *

Department of General Surgery, First Affiliated Hospital of China Medical University, Shenyang, China

ARTICLE INFO

Article history:
Received 26 July 2012
Available online 2 August 2012

Keywords:
CARMA3
NF-κB
Proliferation
Cyclin D1

ABSTRACT

CARMA3 was recently reported to be overexpressed in cancers and associated with the malignant behavior of cancer cells. However, the expression of CARMA3 and its biological roles in colon cancer have not been reported. In the present study, we analyzed the expression pattern of CARMA3 in colon cancer tissues and found that CARMA3 was overexpressed in 30.8% of colon cancer specimens. There was a significant association between CARMA3 overexpression and TNM stage ($p = 0.0383$), lymph node metastasis ($p = 0.0091$) and Ki67 proliferation index ($p = 0.0035$). Furthermore, knockdown of CARMA3 expression in HT29 and HCT116 cells with high endogenous expression decreased cell proliferation and cell cycle progression while overexpression of CARMA3 in LoVo cell line promoted cell proliferation and facilitated cell cycle transition. Further analysis showed that CARMA3 knockdown downregulated and its overexpression upregulated cyclin D1 expression and phospho-Rb levels. In addition, we found that CARMA3 depletion inhibited p-IκB levels and NF-κB activity and its overexpression increased p-IκB expression and NF-κB activity. NF-κB inhibitor BAY 11-7082 reversed the role of CARMA3 on cyclin D1 upregulation. In conclusion, our study found that CARMA3 is overexpressed in colon cancers and contributes to malignant cell growth by facilitating cell cycle progression through NF-κB mediated upregulation of cyclin D1.

1. Introduction

Colorectal carcinoma (CRC) is one of the most prevalent cancers world-wide, and is the third leading cause of cancer-related mortality in the developed countries [1]. The limited ability of conventional therapies to achieve the long-term survival of colon cancer patients suggests the need for new treatment options. CARMA3 (also known as CARD10 or Bimp1) belongs to the CARMA family [2]. Recent studies demonstrated that CARMA3, a scaffold protein, plays critical role in GPCR ligands and PKC-induced NF-κB activation [3–5]. NF-κB activation has been shown to be involved in tumorigenesis and the development of neural, heart and immune diseases [6,7]. PKCa-CARMA3 signaling axis plays an essential role in LPA-induced ovarian cancer cell in vitro invasion [8]. Recent study showed that CARMA3 deficiency impaired cancer cell proliferation in vitro and in vivo and inhibited survival, migration and invasion in MDA468 and A431 cells [8]. CARMA3 knockdown caused marked reduction of SDF-1α mediated invasion of oral squamous cell carcinoma TB2-T4 cells [9]. However, the expression pattern of CARMA3 in human colon cancer has not been explored. In addition, the biological roles of CARMA3 in colon cancer cells are still unclear. To address the above questions, we examined the expression of CARMA3 in colon cancer tissues and its relationship with the clinicopathological parameters by immunohistochemistry. We also examined the biological roles of CARMA3 in colon cancer cell lines and explored its potential mechanism.

2. Materials and methods

2.1. Patients and specimens

The study protocol was approved by the institutional reviewer board of China Medical University. Primary tumor specimens were obtained from 107 patients diagnosed with colon cancer who underwent resection in the First Affiliated Hospital of China Medical University between 2006 and 2008. None of the patients had received radiotherapy or chemotherapy before surgical resection. The histological diagnosis and differentiation grade were evaluated for sections stained with hematoxylin and eosin according to the World Health Organization (WHO) classification guidelines. All 107 specimens were re-evaluated with respect to histological subtype and tumor grade. Tumors were classified into Stage I (21), Stage II (38), Stage III (40), and Stage IV (8) according to WHO guidelines (2007). Fresh specimens including both tumor tissue and corresponding normal tissue were used for RNA and protein extraction immediately after resection.

* Corresponding author. Address: Department of Surgical Oncology and General Surgery, First Hospital of China Medical University, 155 North Nanjing Street, Heping District, Shenyang City 110001, China. Fax: +86 24 23261638.
E-mail address: xuhuimianpaper@yahoo.com.cn (H. Xu).

0006-291X/$ - see front matter © 2012 Elsevier Inc. All rights reserved.
http://dx.doi.org/10.1016/j.bbrc.2012.07.152

2.2. Immunohistochemistry

Surgically excised tumor specimens were fixed with 10% neutral formalin and embedded in paraffin, and 4-μm-thick sections were prepared. Immunostaining was performed using the avidin–biotin–peroxidase complex method (Ultrasensitive™, MaiXin, Fuzhou, China). The sections were deparaffinized in xylene, rehydrated with graded alcohol, and then boiled in 0.01 M citrate buffer (pH 6.0) for 2 min in an autoclave. Hydrogen peroxide (0.3%) was applied to block endogenous peroxide activity and the sections were incubated with normal goat serum to reduce nonspecific binding. Tissue sections were incubated with CARMA3 rabbit polyclonal antibody (1:100 dilution; Sigma, USA) and Ki67 mouse monoclonal antibody (1:200 dilution; Maixin, Fuzhou, China). Staining for both antibodies was performed at room temperature for 2 h. Biotinylated goat antimouse serum IgG was used as a secondary antibody. After washing, the sections were incubated with streptavidin–biotin conjugated with horseradish peroxidase, and the peroxidase reaction was developed with 3,3′-diaminobenzidine tetrahydrochloride. Counterstaining with hematoxylin was performed and the sections were dehydrated in ethanol before mounting.

Two independent blinded investigators examined all tumor slides randomly. Immunostaining of CARMA3was scored on a semiquantitative scale by evaluating in representative tumor areas. Nuclear immunostaining in tumor cells was considered positive staining. We counted 400 tumor cells and calculated the percentage of positively stained cells. The staining intensity was categorized as follows: 0, negative; 1, moderate; and 2, strong. The staining percentage of tumor specimens was scored as 0, 0%; 1 1–5%; 2, 6–25%; 3, 26–75% and 4, 76–100%. The scores of each tumor sample were multiplied to give a final score of 0–8, and the tumor samples with a final score of 4–8 were finally determined as CARMA3 overexpression. According to the recommended classification in previous studies [10], samples with Ki67 nuclear staining equal or above 40% were considered having a high proliferative index, whereas nuclear positivity below 40% was considered a low proliferative index.

2.3. Cell culture and transfection

HT29, HCT116 and LoVo cell lines were obtained from American Type Culture Collection (Manassas, VA, USA). The cells were cultured in DMEM (Invitrogen, Carlsbad, CA, USA) containing 10% fetal calf serum (Invitrogen), 100 IU/ml penicillin (Sigma, St. Louis, MO, USA), and 100 μg/ml streptomycin (Sigma). Cells were grown on sterilized culture dishes and were passaged every 2 days with 0.25% trypsin (Invitrogen).

DharmaFECT1 reagent was used for siRNA transfection (Qiagen, Chicago, IL, USA) according to the manufacturer's instructions. The protein level was assessed 48 h later by western blotting. The ON-TARGETplus CARMA3 siRNA was purchased from Dharmacon (Dharmacon, Lafayette, CO, USA). ON-TARGETplus Non-Targeting siRNA was used as negative control.

The plasmid of pCMV6-CARMA3 was purchased from Origene (Origene, Rockville, USA). Plasmid was transfected into cells using Attractene Transfection (Qiagen, Hilden, Germany). Empty vector was used as a negative control. Cells were harvested 48 h later after transfection.

NF-κB inhibitor BAY 11-7082 was purchased from Sigma (Sigma, USA). Cells was treated at 5 μM concentration for 6 h.

2.4. Western blot analysis

Total proteins from cells were extracted in lysis buffer (Pierce, Rockford, IL) and quantified using the Bradford method. Samples of 50 μg of protein were separated by SDS–PAGE. Samples were transferred to polyvinylidene fluoride membranes (Millipore, Billerica, MA, USA) and incubated overnight at 4 °C with antibody against CARMA3(1:500, Sigma, USA), p-IκB, cyclin D1, CDK4/6, p-Rb (1:1000; Cell signaling, Boston, MA, USA) and a mouse monoclonal antibody against β-actin (1:1000; Santa Cruz). After incubation with peroxidase-coupled antimouse IgG (Santa Cruz) at 37 °C for 2 h, bound proteins were visualized using ECL (Pierce) and detected using a BioImaging System (UVP Inc., Upland, CA, USA).

2.5. Quantitative real-time PCR (SYBR green method)

Total RNA was extracted from cells using Trizol (Qiagen). Reverse transcription of 1 μg of RNA was done using the high capacity cDNA RT kit (Applied Biosystems) following the manufacturer's instructions.

Quantitative real-time PCR was done using SYBR Green PCR master mix (Applied Biosystems) in a total volume of 20 μl on 7900HT fast Real-time PCR system (Applied Biosystems) as follows: 50 °C for 2 min, 95 °C for 10 min, 40 cycles of 95 °C for 15 s, 60 °C for 60 s. The sequences of the primer pairs are as follows: CARMA3forward, 5′ CCCCTAAGAGATCCTTCAGCAG 3′, CARMA3reverse, 5′ CCACACGCTGTCAGAGGATG 3′; cyclin D1 forward, 5′ TATTGCGCTGCTACCGTTGA 3′, cyclin D1 reverse, 5′ CCAATAGCAGCAAACAATGTGAAA 3′. β-actin forward, 5′ ATAGCACAGCCTGGATAGCAACGTAC 3′, β-actin reverse, 5′ CACCTTCTACAATGAGCTGCGTGTG 3′. A dissociation procedure was performed to generate a melting curve for confirmation of amplification specificity. β-actin was used as the reference gene. The relative levels of gene expression were represented as ΔCt = Ct gene –Ct reference, and the fold change of gene expression was calculated by the $2^{-\Delta\Delta Ct}$ Method. Experiments were repeated in triplicate.

2.6. Colony formation and MTT assays

HT29, HCT116 and LoVo cells were transfected for 48 h and then plated into three 6-cm cell culture dishes (1000 per dish) and incubated for 12 days. Plates were washed with PBS and stained with Giemsa. The number of colonies with more than 50 cells was counted. The colonies were manually counted using a microscope.

Cells were plated in 96-well plates in medium containing 10% FBS at approximately 1000 cells per well 24 h after transfection. For quantitation of cell viability, cultures were stained after 4 days in MTT assays. In brief, 20 μl of 5 mg/ml MTT (thiazolyl blue) solution was added to each well and incubated for 4 h at 37 °C. The medium was removed from each well and the resulting MTT formazan was solubilized in 150 μl of DMSO. Each solution was measured spectrophotometrically at 490 nm.

2.7. Luciferase reporter assay

Cells were co-transfected with the firefly luciferase reporter of NF-κB (NF-κB -TA-luc, Beyotime Biotechnology, China) (0.2 μg) along with the Renilla luciferase reporter (Promega, USA) (0.02 μg) using Attractene reagent (Qiagen, Hilden, Germany). After 24 h, the luciferase activity was measured in the cellular extracts using a dual luciferase reported gene assay kit (Promega, CA, USA). The relative activity of reporter gene was calculated by dividing signals of NF-κB luciferase reporter by signals obtained from Renilla luciferase reporter.

2.8. Statistical analysis

SPSS version 11.5 for Windows was used for all statistical analyses. Chi-Square test was used to evaluate possible correlations between CARMA3 overexpression and clinicopathologic factors. Student's *t*-test was used to compare densitometry data on focus numbers between control and transfected cells. All p values were based on the two-sided statistical analysis and $p < 0.05$ was considered to be statistically significant in difference.

3. Results

3.1. Expression and distribution of CARMA3 in normal colon tissue and colon cancer specimens

In order to investigate CARMA3protein levels in colon cancer, a panel of 107 primary colon cancer samples as well as normal colon tissues was studied by immunohistochemistry and we found that all the CARMA3 protein was apparently localized in the cytoplasmic compartment. None or weak expression of CARMA3 was detected in normal colon tissue (Fig. 1A). Moderate or strong cytoplasmic staining with a final score of 4–8 was considered as CARMA3 overexpression (Fig. 1C–D). We detected the overexpression of CARMA3 in 33 out of 107 (30.8%) colon cancer tissues.

The relationship between the CARMA3expression and the clinical parameters was analyzed. As shown in Table 1, no statistical difference was found between the positive CARMA3expression and the characteristics of age ($p = 0.4433$), gender ($p = 0.7352$), tumor status ($p = 0.2621$) and tumor differentiation ($p = 0.4226$). CARMA3 overexpression correlated with advanced TNM stage ($p = 0.0383$), positive nodal metastasis ($p = 0.0091$) and distal metastasis ($p = 0.0438$). The level of CARMA3 expression in stage IV colon cancers (62.50%) was higher than in stage III (40.00%), stage II (21.05%) and stage I (19.05%) colon cancers. In addition, CARMA3 overexpression correlated with strong Ki-67 signals ($p = 0.0035$), (Fig. 1E–H). To validate the immunohistochemical results, we performed western blot and realtime RT-PCR in 8 cases of primary colon cancer tissues (*T*) and adjacent noncancerous tissues. We found that CARMA3 expression in 3 cases of cancer tissues were much higher than that in normal tissues (Fig. 1I).

3.2. CARMA3 depletion inhibits colon cancer cell proliferation and its overexpression promotes proliferation

We detected CARMA3 expression levels in five colon cancer cell lines by western blot and realtime PCR analysis. We found high level of CARMA3 expression in HT29, HCT116 and SW480 cell lines and low CARMA3 level in LoVo and HCT8 cell lines (Fig. 1J). In order

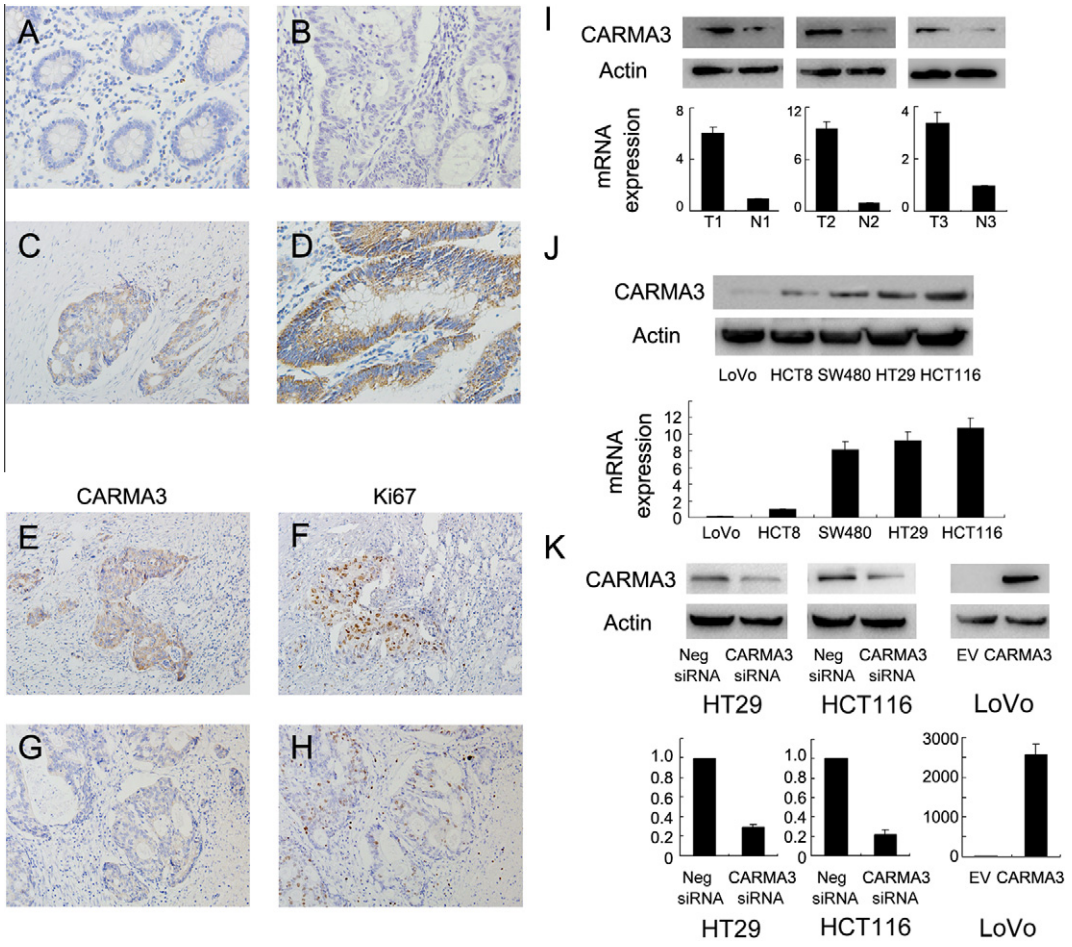

Fig. 1. Expression of CARMA3 protein in colon cancer tissues and cell lines. (A). Negative staining in normal colon mucosa. (B). Negative CARMA3 staining in colon cancer. (C). Moderate cytoplasmic CARMA3 expression in colon cancer. (D). Strong cytoplasmic staining of CARMA3 in colon cancer. (E, F, G and H). Correlation of CARMA3 expression with high Ki67 proliferation index. Case that has a high level of CARMA3 expression (E) shows a high proliferation index indicated by high Ki-67 label (F), whereas, the case with negative reactivity to CARMA3 (G) has a low proliferation index (H). (Magnification, 200X). (I). Western blot and Realtime PCR analysis of CARMA3 overexpression in three colon cancer specimens (T1, T2, T3) and adjacent non-neoplastic specimens (N1, N2, N3). (J). Protein and mRNA expression of CARMA3 in colon cancer cell lines. HCT116 and HT29 cell line have relatively high expression and LoVo cell line has relatively low expression. (K). Western blot and realtime PCR analysis showed that siRNA treatment markedly decreases CARMA3 levels in HT29 and HCT116 cells and CARMA3 transfection significantly increased its expression in LoVo cells.

Table 1
Distribution of CARMA3 status in colorectal cancer according to clinicopathological characteristics.

Characteristics	Number of patients	Rsf-1 low expression	Rsf-1 overexpression	*P*
Age				
Female	46	30(65.22%)	16(34.78%)	0.4433
Male	61	44(55.74%)	17(44.26%)	
Gender				
<60	59	40(67.80%)	19(32.20%)	0.7352
⩾60	48	34(70.83%)	14(29.17%)	
TNM stage				
I	21	17(80.95%)	4(19.05%)	0.0383
II	38	30(78.95%)	8(21.05%)	
III	40	24(60.00%)	16(40.00%)	
IV	8	3(37.50%)	5(62.50%)	
Tumor status				
T1 T2	27	21(77.78%)	6(22.22%)	0.2621
T3 T4	80	53(66.25%)	27(33.75%)	
Nodal status				
N0	59	42(79.66%)	12(20.34%)	0.0091
N1 N2 N3	48	27(56.25%)	21(43.75%)	
Distant metastasis				
Absent	99	71(71.72%)	28(28.28%)	0.0438
Present	8	3(73.50%)	5(62.50%)	
Differentiation				
Poor	24	15(62.50%)	9(37.50%)	0.4226
Moderate + Well	83	59(71.08%)	24(28.92%)	
Ki67 status				
Low	45	38(84.44%)	7(15.56%)	0.0035
High	62	36(58.06%)	25(41.94%)	

to investigate the biological roles of CARMA3 in colon cancer cells, we employed a pool consisting of three CARMA3-targeting siRNAs in HT29 and HCT116 cell lines. We also overexpressed CARMA3 in LoVo cell line using pCMV6-CARMA3 plasmid. Using western blot and realtime PCR analysis, we confirmed the CARMA3 knockdown and transfection efficiency (Fig. 1K). Next, we tested the effects of CARMA3 depletion and overexpression on proliferation ability of colon cancer cells. The proliferation rate was determined by MTT assay. We found that treatment of CARMA3-specific siRNA resulted in a significant decrease in proliferation compared with control siRNA while its overexpression enhanced its growth rate (Fig. 2A). To validate this effect in colon cancer cells by an independent method, we performed colony formation assay. In accordance with the MTT results, colony formation assay showed that CARMA3 knockdown in HT29 and HCT-116 cells led to strong reduction of focus numbers (Negative Control vs CARMA3siRNA, HT29: 154 ± 11 vs 80 ± 7, $p < 0.05$; HCT116: 309 ± 12 vs 109 ± 16, $p < 0.05$, Fig. 2B). CARMA3 overexpression increased colony formation ability in LoVo cells (HCT116: 129 ± 10 vs 195 ± 21, $p < 0.05$, Fig. 2B).

3.3. Depletion of CARMA3 facilitates G1/S transition and upregulates cyclin D1 and p-Rb levels in colon cancer cells

To examine the possible mechanisms of CARMA3 depletion on tumor proliferation, we overexpressed CARMA3 in LoVo cells and down-regulated CARMA3 in HT29 and HCT116 cells and then performed cell cycle analysis. We found that the percentage of G1 phase was decreased in CARMA3 overexpressed LoVo cells (EV vs CARMA3: 62.7 ± 0.5 vs 52.3 ± 1.1, $p < 0.05$) and increased in CARMA3 depleted cells (Negative Control vs CARMA3siRNA, HT29: 50.8 ± 1.8 vs 60.9 ± 1.2, $p < 0.05$; HCT116: 43.7 ± 2.5 vs 54.0 ± 1.4, $p < 0.05$, Fig. 2C), whereas the percentage of S phase was increased in LoVo with CARMA3 transfection (EV vs CARMA3: 22.6 ± 0.6 vs 30.3 ± 2.5, $p < 0.05$) and decreased in these cells with siRNA treatment (Negative Control vs CARMA3siRNA, HT29: 40.7 ± 1.1 vs 33.1 ± 1.2, $p < 0.05$; HCT116: 36.1 ± 1.3 vs 28.3 ± 1.9, $p < 0.05$, Fig. 2C). These results indicated that CARMA3 induces cell cycle progression at the G1/S boundary.

We further tested the effect of CARMA3 knockdown and overexpression on several cell cycle related factors. As shown in Fig. 3, knockdown of CARMA3 decreased the protein and mRNA levels of cyclin D1 in both HT29 and HCT116 cell lines while CARMA3 overexpression upregulated cyclin D1 in LoVo cell line. The levels of CDK4/6 expression were not changed. In addition, Depletion of CARMA3 resulted in phospho-Rb reduction and its overexpression increased phospho-Rb expression. Together, these results suggested that CARMA3 affects cell cycle progression by regulating cyclin D1 expression in colon cancer cells.

3.4. CARMA3 reuglates cyclinD1 expression through NF-κB pathway activation

Since CARMA3 was reported to be involved in NF-κB activation and cyclinD1 was NF-κB downstream target, we asked if CARMA3 regulates cyclin D1 by activation of NF-κB pathway. We checked expression of p-IκB and NF-κB luciferase activity. We found that the level of p-IκB was upregulated in CARMA3 transfected LoVo cells (Fig. 3B) and downregulated in CARMA3 depleted HT29 and HCT116 cells (Fig. 3A). On the other hand, CARMA3 overexpression upregulated NF-κB reporter luciferase activity and CARMA3 depletion inhibited its activity. The above results suggested the possible involvement of NF-κB activation in CARMA3 induced cyclin D1 upregulation. To confirm this, we employed NF-κB inhibitor BAY 11-7082 (5 μM, 6 h) to block NF-κB activity in CAMRA3 transfected LoVo cells. As shown in Fig. 3, NF-κB inhibitor reversed the upregulation cyclinD1 expression after CARMA3 overexpression.

4. Discussion

Constitutive activation of NF-κB has been described in a great number of solid tumors, which support cancer cell proliferation and survival [11,12]. As a NF-κB regulatory protein, the role of CARMA3 has been explored in several cancers [8,13]. However, its expression pattern and biological roles in colon cancer have not been explored. We demonstrated that the level of CARMA3 in colon cancer tissues was significantly higher than that in normal colon tissues. In addition, there were correlations between CARMA3 up-regulation and tumor stage, nodal status and Ki67 proliferation index, suggesting CARMA3 might associate with colon cancer progression.

To explore the relationship between CARMA3 and the biological behavior of colon cancer cells, we blocked CARMA3 function by using siRNA treatment in the HT29 and HCT116 cell lines which have high endogenous CARMA3 expression. We found that CARMA3 depletion caused an obvious decrease in the proliferation rate and colony formation ability in both cell lines, which was in accordance with our immunohistochemical data and previous studies [13]. To find out the potential mechanisms of CARMA3 on cell proliferation, we examined the effects of CARMA3 knockdown and overexpression on cell cycle progression. We found that in the colon cancer cell lines HT29 and HCT116, CARMA3 knockdown inhibited G1/S progression while CARMA3 overexpression in HT29 cell line facilitated G1/S transition. Cyclin D1 interacts with Cdk4/6 to carry out its function. Cyclin D-Cdk4/6 complex partially phosphorylates Rb, which is important for cell cycle progression [14,15]. In the present study, we found that knockdown of CARMA3 decreased the protein levels of Cyclin D1, p-Rb and CAMRA3 overexpression increased cyclin D1 and p-Rb expression. These findings indicated that CARMA3 induced colon cancer proliferation by cyclin D1 upregulation.

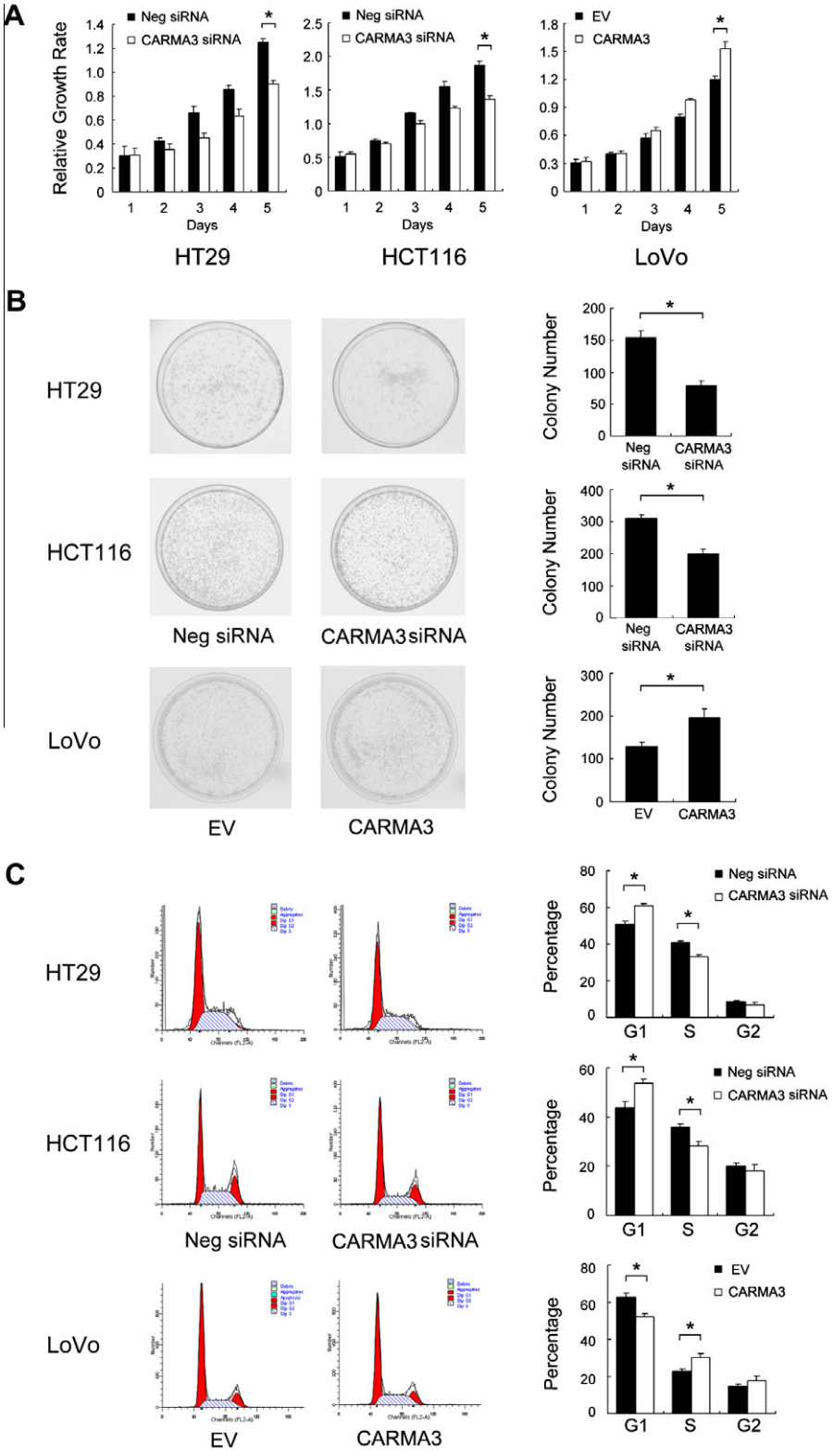

Fig. 2. CARMA3 knockdown inhibited and CARMA3 overexpression promoted cell proliferation and cell cycle progression in colon cancer cell lines. (A). MTT assay showed that CARMA3 knockdown inhibited proliferation in HT29 and HCT116 cell lines (Day5: $p < 0.05$). CARMA3 overexpression promoted proliferation in LoVo cell line (Day5: $p < 0.05$). (B). Colony formation assay was performed in cells transfected with CARMA3 siRNA and CARMA3 plasmid. A decrease in colony formation was seen in the groups with siRNA treatment in HT29 and HCT116 cell lines ($p < 0.05$). CARMA3 transfection increased colony number in LoVo cells ($p < 0.05$). (C). CARMA3 knockdown increased G1 phase cells (HT29, control vs CARMA3 siRNA, 50.8 ± 1.8 vs 60.9 ± 1.2, $P < 0.05$; HCT116, control vs CARMA3 siRNA, 43.7 ± 2.5 vs 54.0 ± 1.4, $P < 0.05$) and decreased S phase cells (HT29, control vs CARMA3 siRNA, 40.7 ± 1.1 vs 33.1 ± 1.2; HCT116, control vs CARMA3 siRNA, 36.1 ± 1.3 vs 28.3 ± 1.9, $P < 0.05$). CARMA3 overexpression increased S phase cells (LoVo, EV vs CARMA3, 22.6 ± 0.6 vs 30.3 ± 2.5, $P < 0.05$) and decreased G1 phase cells (LoVo, EV vs CARMA3, 62.7 ± 0.5 vs 52.3 ± 1.1, $p < 0.05$).

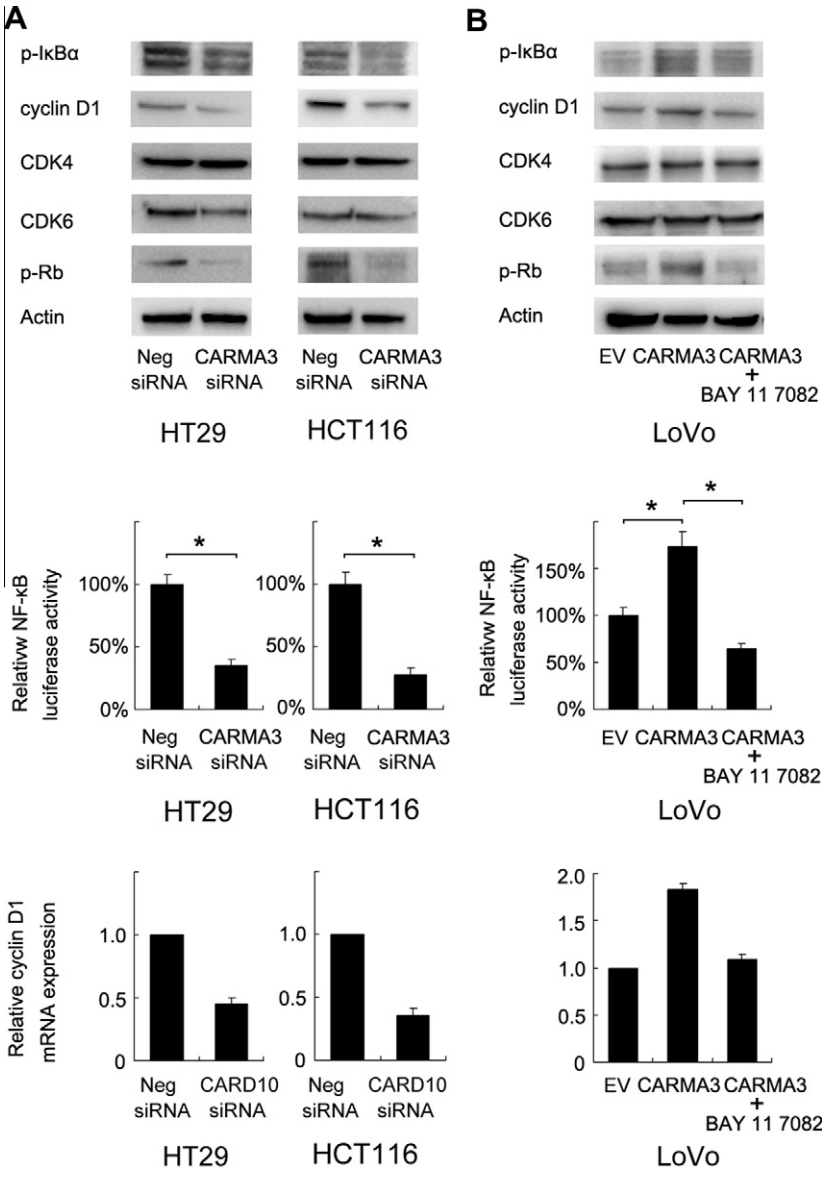

Fig. 3. CARMA3 knockdown decreased and CARMA3 overexpression increased cyclinD1, p-Rb and p-IκB expression and NF-κB luciferase activity. A. Western blotting analysis revealed that knockdown of CARMA3 decreased the levels of cyclin D1 mRNA and protein, p-Rb and p-IκB in both HT29 and HCT116 cell lines, without significant changes in CDK4 and CDK6 protein expression. CARMA3 depletion also inhibited NF-κB luciferase activity. B. CARMA3 overexpression increased the levels of cyclin D1, p-Rb, p-IκB and NF-κB luciferase activity in LoVo cells. NF-κB inhibitor BAY 11-7082 blocked NF-κB activity and cyclin D1 upregulation in CAMRA3 transfected LoVo cells.

Activation of NF-κB pathway has been showed to play an important role in tumor progression in various types of cancers. CARMA3/NF-κB signaling axis has been confirmed in many types of diseases such as cancer and atherogenesis [16,17]. In ovarian cancer cell lines, knockdown of CARMA3 abolishes LPA receptor-induced NF-κB activation, and reduces LPA-induced ovarian cancer invasion [8]. In vascular smooth cells, downregulation of CARMA3 substantially impairs Ang-II-receptor-induced NF-κB activation [5]. Recently, it was found that CARMA3 was crucial for EGFR-induced activation of NF-κB [13]. In the present study, we demonstrated a link between CARMA3 and NF-κB activation in colon cancer cells. We found that CARMA3 depletion inhibited p-IκB level and NF-κB activity and its overexpression increased p-IκB expression and NF-κB activity. It was reported that NF-κB activation could result in transcription activation of cyclin D1 [18,19]. To confirm the relationship between CARMA3, cyclin D1 and NF-κB activation, we employed NF-κB inhibitor BAY 11-7082 to treat CARMA3 transfected cells. We found that NF-κB inhibition reversed the role of CARMA3 on cyclin D1, suggesting CARMA3 could induce cyclin D1 expression via NF-κB activation.

In conclusion, our study found that CARMA3 overexpression existed in colon cancer and correlated with TNM stage, nodal metastasis and proliferation index. CARMA3 contributed to the malignant cell growth by facilitating cell cycle progression through NF-κB mediated upregulation of cyclin D1. These results suggested that CARMA3 functions as a positive regulator of colon cancer proliferation.

Conflict of interest

No potential conflicts of interest were disclosed.

References

[1] R. Siegel, D. Naishadham, A. Jemal, Cancer statistics, CA Cancer J. Clin. 62 (1) (2012) 10–29.

[2] L. Wang, Y. Guo, W.J. Huang, X. Ke, J.L. Poyet, G.A. Manji, S. Merriam, M.A. Glucksmann, P.S. DiStefano, E.S. Alnemri, J. Bertin, Card10 is a novel caspase recruitment domain/membrane-associated guanylate kinase family member that interacts with BCL10 and activates NF-kappa B, J. Biol. Chem. 276 (24) (2001) 21405–21409.
[3] L.M. McAllister-Lucas, N. Inohara, P.C. Lucas, J. Ruland, A. Benito, Q. Li, S. Chen, F.F. Chen, S. Yamaoka, I.M. Verma, T.W. Mak, G. Nunez, Bimp1, a MAGUK family member linking protein kinase C activation to Bcl10-mediated NF-kappaB induction, J. Biol. Chem. 276 (33) (2001) 30589–30597.
[4] B.C. Grabiner, M. Blonska, P.C. Lin, Y. You, D. Wang, J. Sun, B.G. Darnay, C. Dong, X. Lin, CARMA3 deficiency abrogates G protein-coupled receptor-induced NF-{kappa}B activation, Genes Dev. 21 (8) (2007) 984–996.
[5] L.M. McAllister-Lucas, J. Ruland, K. Siu, X. Jin, S. Gu, D.S. Kim, P. Kuffa, D. Kohrt, T.W. Mak, G. Nunez, P.C. Lucas, CARMA3/Bcl10/MALT1-dependent NF-kappaB activation mediates angiotensin II-responsive inflammatory signaling in nonimmune cells, Proc. Natl. Acad. Sci. U S A 104 (1) (2007) 139–144.
[6] B.B. Aggarwal, Nuclear factor-kappaB: the enemy within, Cancer Cell 6 (3) (2004) 203–208.
[7] M.S. Hayden, S. Ghosh, Signaling to NF-kappaB, Genes Dev. 18 (18) (2004) 2195–2224.
[8] C. Mahanivong, H.M. Chen, S.W. Yee, Z.K. Pan, Z. Dong, S. Huang, Protein kinase C alpha-CARMA3 signaling axis links Ras to NF-kappa B for lysophosphatidic acid-induced urokinase plasminogen activator expression in ovarian cancer cells, Oncogene 27 (9) (2008) 1273–1280.
[9] A.O. Rehman, C.Y. Wang, CXCL12/SDF-1 alpha activates NF-kappaB and promotes oral cancer invasion through the Carma3/Bcl10/Malt1 complex, Int. J. Oral Sci. 1 (3) (2009) 105–118.
[10] C.J. Allegra, S. Paik, L.H. Colangelo, A.L. Parr, I. Kirsch, G. Kim, P. Klein, P.G. Johnston, N. Wolmark, H.S. Wieand, Prognostic value of thymidylate synthase, Ki-67, and p53 in patients with Dukes' B and C colon cancer: a national cancer institute-national surgical adjuvant breast and bowel project collaborative study, J. Clin. Oncol. 21 (2) (2003) 241–250.
[11] G. He, G.Y. Yu, V. Temkin, H. Ogata, C. Kuntzen, T. Sakurai, W. Sieghart, M. Peck-Radosavljevic, H.L. Leffert, and M. Karin, Hepatocyte IKKbeta/NF-kappaB inhibits tumor promotion and progression by preventing oxidative stress-driven STAT3 activation. Cancer Cell. 17 (3) (2010) 286–97.
[12] S. Umar, S. Sarkar, S. Cowey, P. Singh, Activation of NF-kappaB is required for mediating proliferative and antiapoptotic effects of progastrin on proximal colonic crypts of mice, in vivo, Oncogene 27 (42) (2008) 5599–5611.
[13] T. Jiang, B. Grabiner, Y. Zhu, C. Jiang, H. Li, Y. You, J. Lang, M.C. Hung, and X. Lin, CARMA3 is crucial for EGFR-Induced activation of NF-kappaB and tumor progression. Cancer Res. 71 (6) (2011) 2183–92.
[14] J.K. Kim, J.A. Diehl, Nuclear cyclin D1: an oncogenic driver in human cancer, J. Cell Physiol. 220 (2) (2009) 292–296.
[15] K.E. Knudsen, J.A. Diehl, C.A. Haiman, E.S. Knudsen, Cyclin D1: polymorphism, aberrant splicing and cancer risk, Oncogene 25 (11) (2006) 1620–1628.
[16] J. Sun, CARMA3: A novel scaffold protein in regulation of NF-kappaB activation and diseases. World, J Biol Chem. 1 (12) (2010) 353–61.
[17] L.M. McAllister-Lucas, X. Jin, S. Gu, K. Siu, S. McDonnell, J. Ruland, P.C. Delekta, M. Van Beek, and P.C. Lucas, The CARMA3-Bcl10-MALT1 signalosome promotes angiotensin II-dependent vascular inflammation and atherogenesis. J Biol Chem. 285 (34) (2010) 25880–4.
[18] S.G. Park, C. Chung, H. Kang, J.Y. Kim, G. Jung, Up-regulation of cyclin D1 by HBx is mediated by NF-kappaB2/BCL3 complex through kappaB site of cyclin D1 promoter, J. Biol. Chem. 281 (42) (2006) 31770–31777.
[19] W. Ouyang, Q. Ma, J. Li, D. Zhang, Z.G. Liu, A.K. Rustgi, C. Huang, Cyclin D1 induction through IkappaB kinase beta/nuclear factor-kappaB pathway is responsible for arsenite-induced increased cell cycle G1-S phase transition in human keratinocytes, Cancer Res. 65 (20) (2005) 9287–9293.